Nanoscale

ARTICLE

Impact of covalent functionalization by diazonium chemistry on the electronic properties of graphene on SiC

Received 00th January 20xx,
Accepted 00th January 20xx

DOI: 10.1039/x0xx00000x

G. Ambrosio[a,b], A. Brown[b], L. Daukiya[b], G. Drera[a], G. Di Santo[c], L. Petaccia[c], S. De Feyter[b], L. Sangaletti[a], and S. Pagliara[a].

Plenty of strategies focused on covalent interaction have been developed to functionalize the graphene surface in order to employ it in a wide range of applications. Among them, the use of radical species including nitrene, carbene and aryl diazonium salts is regarded as a promising strategy to establish covalent functionalization of graphene. In this work we highlight the effect of the diazonium chemistry on the electronic properties of graphene on SiC. On the basis of X-ray and synchrotron-based photoemission experiments we are able to prove that the 3,4,5-trimethoxybenzenediazonium (TMeOD) units, reduced and chemisorbed onto graphene by using electrochemistry, preserve the electronic structure of the Dirac cone, though inducing an n-type doping of graphene, as revealed by a downshift of the Dirac cone probed by angle-resolved photoemission experiments.

Introduction

The past decade has witnessed an overwhelming research towards exploring the novel fundamental physical properties of graphene[1] along with development of new methods for its synthesis supported on variety of substrates[2]. However, in order to fully harness the potential of graphene[3] it is of outmost importance to develop methods for a controlled tuning of its physical and chemical properties. Functionalization by atoms and molecules has been studied as a promising approach to modify the intrinsic properties of graphene. In this regard, numerous experimental methods such as non-covalent and covalent functionalization by organic molecules[4-6], as well as intercalation by atoms and molecules[7] have been developed to engineer the electronic band structure of graphene. Covalent functionalization by molecules however is by far the most *promising* approach as it allows for a robust and stable functionalization at atmospheric conditions therefore causing the most significant change in the electronic band structure of graphene[8, 9]. Several experimental and theoretical[10, 11] studies have revealed that covalent functionalization of graphene by reactive molecules results in chemisorption (grafting hereafter) of molecules on graphene lattice by forming a covalent bond, where the rehybridization of sp^2 carbons of graphene in sp^3 at the grafting sites takes place. Different reaction methods such as free radical addition, cycloaddition, nucleophilic addition, substitution and rearrangement reactions have been developed for covalent functionalization of pristine graphene[12]. Free radical addition approach using diazonium salts is one of the most studied methods[13] for covalent functionalization, as this approach results in a high degree of functionalization.

Aryl diazonium molecules react with graphene via an electron transfer mechanism[14], in which the delocalized electrons of graphene are transferred to diazonium cations, resulting in the formation of aryl radicals and in the release of N_2 molecules. The aryl radical then reacts with a carbon atom of the graphene lattice and gives rise to the covalent bond (Fig. 1).

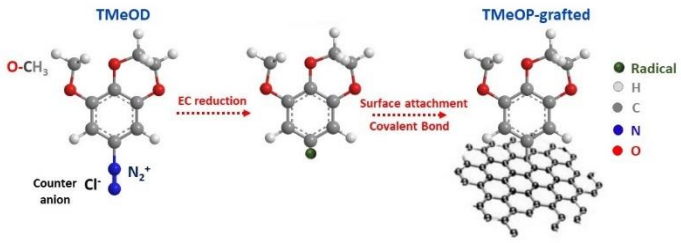

Fig. 1: Schematic of the covalent modification of graphene using aryl diazonium molecules, in particular 3,4,5-trimethoxybenzene diazonium (TMeOD). The diazonium compound is activated in the electrochemical cell (EC reduction), resulting in the formation of a radical that attaches to the graphene lattice creating a covalent bond.

a. I-LAMP and Dipartimento di Matematica e Fisica, Università Cattolica del Sacro Cuore, Via dei Musei 41, 25121 Brescia, Italy.
b. Division of Molecular Imaging and Photonics, Department of Chemistry, KU Leuven, Celestijnenlaan 200F, 3001 Leuven, Belgium.
c. Elettra Sincrotrone Trieste, Strada Statale 14 km 163.5, 34149 Trieste, Italy.

† Footnotes relating to the title and/or authors should appear here.
Electronic Supplementary Information (ESI) available: [details of any supplementary information available should be included here]. See DOI: 10.1039/x0xx00000x

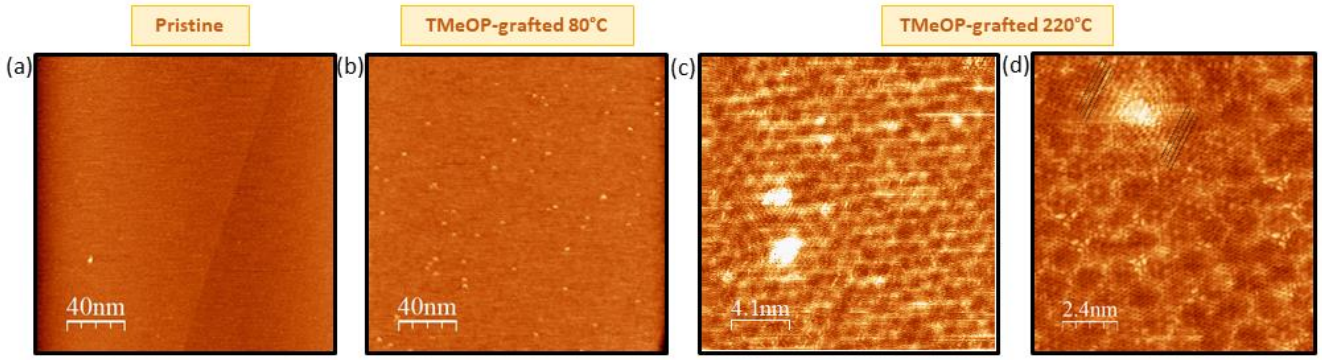

Fig. 2: 200 nm x 200 nm STM images of (a) pristine graphene on SiC and (b) 1 mM TMeOP-grafted units on graphene after an annealing at 80°C in UHV, acquired at I_{set} = 50 pA and V_{bias} = -0.3 V. (c) 20.5 nm x 20.5 nm and (d) 12 nm x 12 nm STM images after an annealing at 220°C in UHV.

Diazonium molecules with different electron withdrawing or donating functional groups have been successfully grafted on graphite and graphene[15]. Depending on the electron donating or withdrawing nature of the functional groups on diazonium molecules, a robust and stable n-type or p-type doping of graphene should occur. Although a number of studies on diazonium grafted graphene suggested a modification of electronic band structure of graphene, only a few show a clear modification of electronic band structure by means of angle-resolved ultraviolet photoelectron spectroscopy (ARPES)[16]. In this study we combine surface characterization techniques such as X-Ray Photoemission Spectroscopy (XPS) and Scanning Tunnelling Microscopy (STM) with ARPES where we show the impact of functionalization on the electronic band structure of graphene before and after the covalent grafting of diazonium molecules. Covalent functionalization by TMeOP-grafted units (3,4,5 trimethoxyphenyl-units, Fig. 1) results in a stable n-type doping of graphene as evidenced by ARPES measurements.

Results and discussion

To confirm the grafting of the TMeOP units on the graphene-SiC, we perform STM measurements (Fig. 2). After the functionalization and an annealing at 80°C in UHV, bright structures are observed, not present in the pristine graphene-SiC sample, with an average height of 0.5 nm (Fig. 2a and Fig. 2b). In agreement with literature[13, 15], we can assign these features to covalently bound species and we can give an estimation of the density of grafted units from the STM images[17], which results to be $\rho = (2.5 \pm 0.13) \cdot 10^{-3}$ molecules·nm^{-2} (Fig. 2b). The distribution of the bright structures suggests that graphene is randomly grafted by TMeOP. After an annealing at 220°C, the number of bright features related to the grafted units appears to be reduced and we can also observe the distortion of the graphene lattice caused by the sp^3 defects with STM[13], as shown in Fig. 2c and 2d.

Raman measurements show an increase of I_D/I_G intensity ratio (Supplementary Information, Fig. S1 †) which can be ascribed to the formation of sp^3 sites[18, 19], confirming the covalent functionalization of graphene by TMeOP units in agreement with earlier studies conducted on similar radicals[15]. To further evaluate the impact of covalent functionalization on the electronic properties of graphene, we carried out XPS measurements. The wide XPS spectra for pristine monolayer graphene on SiC (0001) and 1 mM TMeOP-grafted graphene are shown in Supplementary Information (Fig. S2†).

The chemical environment before and after the graphene functionalization is investigated by collecting the C 1s core level (Fig. 3). Pristine graphene spectra were fitted by five components (Fig. 3a). The first at lowest binding energy BE = 283.67 eV is ascribed to the SiC substrate[20], while the main peak (C-sp^2) at BE = 284.66 eV is ascribed to the sp^2 hybridized carbon atoms of the graphene layer. Two additional components labelled as S1 and S2 can be identified at BE = 285.06 eV and BE = 285.66 eV, respectively. According to Riedl et al.[21], S1 results from C atoms of the buffer layer bound with one Si atom of the SiC(0001) and three C atoms in the sp^2 buffer layer. The S2 component comes from the sp^2 carbon atoms of the buffer layer not bonded with SiC since not all the C atoms of the buffer layer form a bond with Si due to the lattice mismatch. The energy position and the intensity ratio of these peaks are set to be in agreement with previous studies on graphene-SiC[21, 22]. The component at higher BE = 287.01 eV is associated with the oxygen contamination, C-O**.** Here, it is reasonable to consider that the grafting of aryl units takes place only on graphene and there is no modification of the underlying buffer layer resulting from the functionalization process. Indeed, the binding energy and the intensity ratio of the S1 and S2 feature with respect to the SiC component can be considered comparable with those of the pristine graphene-SiC[23]. After the functionalization the C 1s spectrum of graphene is somewhat modified, as shown in Fig. 3b. An increase in the intensity of C-sp^2 component is observed which can be ascribed to additional C-sp^2 signal coming from the carbon

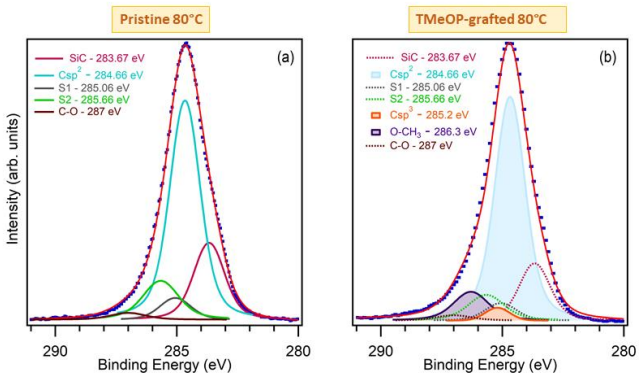

Fig. 3 : XPS spectra of (a) pristine graphene- SiC and (b) 1 mM TMeOP-grafted on graphene-SiC. Both spectra were acquired after an annealing at 80°C, i.e. below the desorption temperature of the grafted units.

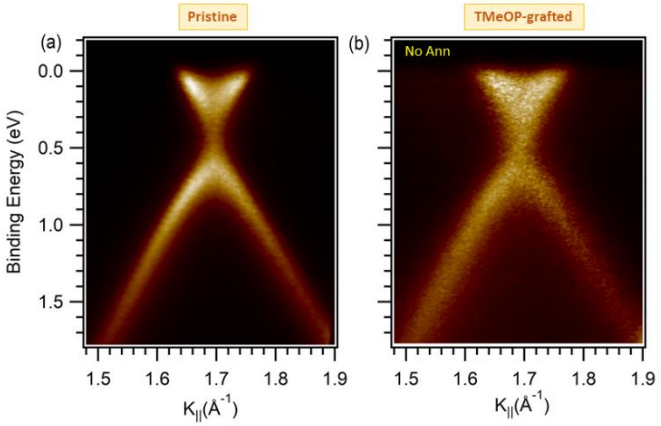

Fig. 4: ARPES map of the Dirac cone of graphene-SiC (a) before and (b) after the functionalization by 1 mM TMeOP units. The pristine substrate was annealed at 600°C while the ARPES map of the functionalized sample was acquired without annealing.

atoms of the phenyl rings of the TMeOP-grafted units. The C-sp^3 peak, associated to the sp^3 hybridized carbon atoms of the functionalized graphene-SiC is at BE = 285.20 eV. Deconvolution also reveals a peak at BE = 286.30 eV which can be ascribed to the O-CH_3 groups of TMeOP-grafted units. In the fitting procedure, the ratio between the O-C and to C-sp^3 spatial features results to be about six in agreement with the stoichiometry of TMeOP-grafted unit.

Fig. 4a shows the dispersion of the π-bands measured by ARPES on pristine graphene around the K-point along the ΓKM high symmetry direction of the Brillouin zone. The position of the Dirac point is downshifted by about 400 meV with respect to the Fermi level due to an intrinsic n-type doping of graphene as a result of charge transfer from underlying SiC(0001) substrates[22, 24, 25]. The photoemission intensity around the Dirac point is originated from the interlayer coupling between graphene and the SiC buffer layer[26, 27].

Fig. 4b shows the ARPES spectra of functionalized graphene of the same sample, it is to be noted that the sample was not annealed prior to collecting the spectra. Two important results come out, firstly a downshift of the Dirac point at binding energy of about 450 meV, indicating an additional n-type doping of the functionalized graphene with respect to the pristine case. Secondly, the ARPES spectra do not show any sign of band gap opening as expected for covalent modification of graphene[13]. We note that the absence of a band gap could be due to the random grafting of the units on graphene-SiC observed by STM and/or to the low concentration of the grafted units[28].

The doping level of graphene can be assessed through an analysis of the π-band dispersion around the K point of the Brillouin zone. Considering that the presence of the Dirac cone elongation (neck) hinders a direct estimation of the Dirac point position, we have firstly extracted the binding energies of the photoemission intensity maxima of selected momentum distribution curves (blue dots in Fig. 5) and then we applied a linear fit procedure (black line) in order to localize the Dirac point. From the intersection point of the linear fits, the position of the Dirac point is at (416 ± 8) meV and (450 ± 9) meV for the pristine and grafted graphene–SiC, respectively. We note that the further shift of the Dirac point from the Fermi level, corresponding to an increased n-type doping of the grafted graphene, cannot be ascribed to ambient contamination as oxygen adsorption on graphene induces a p-type doping of graphene as reported in literature[29-32].

To further confirm this result, we have collected ARPES measurements after different annealing temperatures of the sample and, as expected, a shift of the Dirac cone toward the pristine condition takes place due to the desorption of the aryl units (Fig. 5). The ARPES spectra, in particular, were acquired after the annealing at 140°C and 220°C and the Dirac point was observed (408 ± 8) and (409 ± 8) meV, respectively (Fig. 5b and 5c) by following the procedure previously described. The recovery toward the initial energy position can be related to the molecule desorption that takes place at about 120°C[33, 34].

From the slope of the linear dispersion of the binding energy versus the k-momentum (Fig. 5a and 5b), it is possible to obtain the Fermi velocity of the electrons along the ΓK and KM high symmetry directions. The velocity values are (1.14 ± 0.05)·10^6 m/s and (1.07± 0.05)·10^6 m/s for the pristine, and (1.04 ± 0.05)·10^6 m/s and (1.09 ± 0.05)·10^6 m/s for the the grafted graphene. The agreement of the two Fermi velocities within the error bars confirms that the graphene electronic properties do not change significantly after the grafting procedure.

From the energy shift of the Dirac point and considering that the TMeOP-grafted units do not form a multilayer, we are able to estimate the electron-donating capability of the TMeOP-grafted units[15, 35]. In particular, we acquired ARPES data versus azimuthal

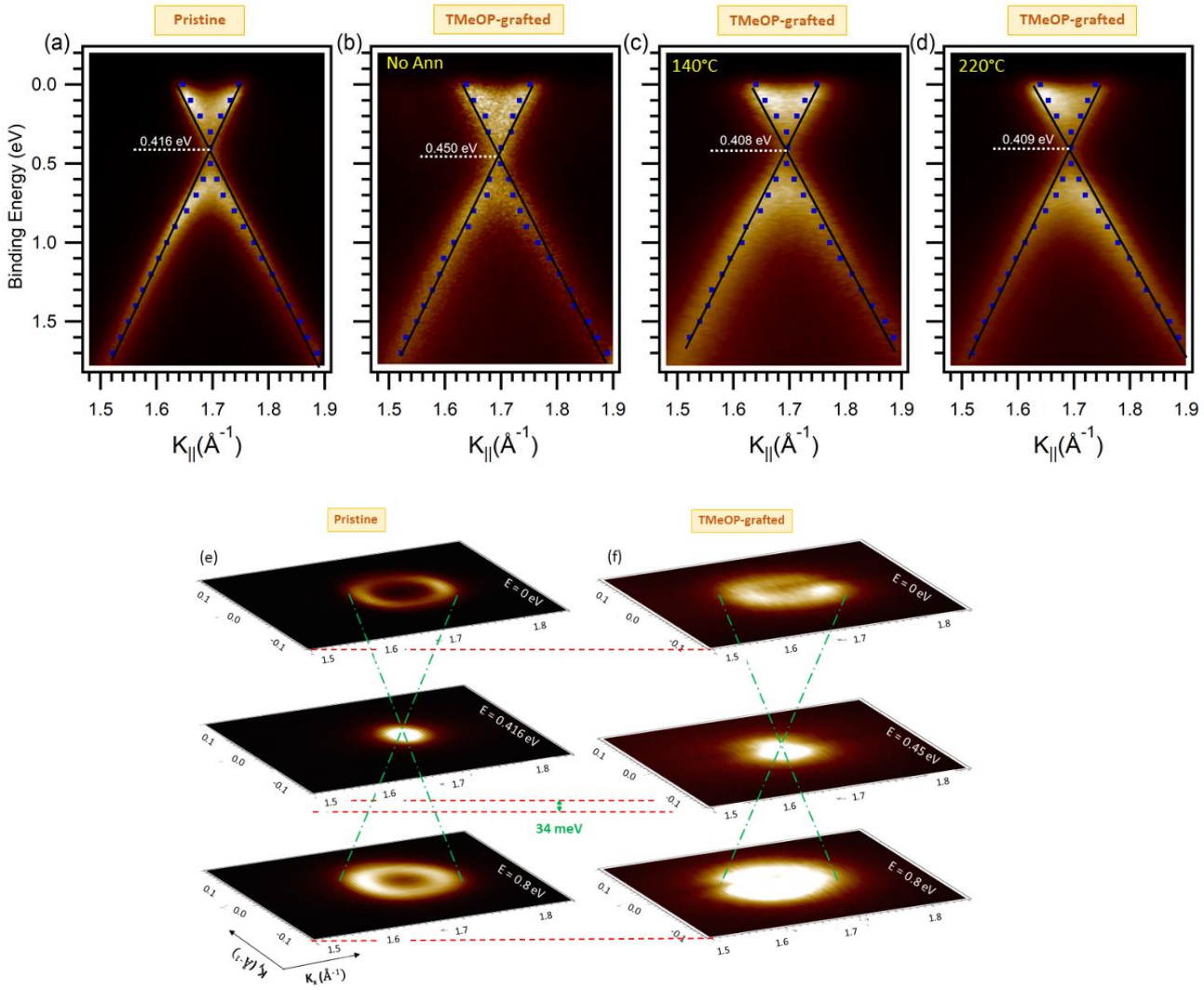

Fig.5: ARPES map of the Dirac cone of graphene around the K point and along the ΓKM direction of the Brillouin zone on (a) pristine SiC annealed at 600°C, (b) after the functionalization by 1 mM TMeOP without any annealing. ARPES maps of the functionalized sample after an annealing at (c) 140°C and (d) 220°C. (e) – (f) Constant energy maps of the Dirac cone in (a)-(b), respectively taken at the Fermi level and at the binding energies reported in the figure. The dashed green lines are a guide for the eyes.

angle around the K point of the Brillouin zone before and after the grafting procedure.

In Fig. 5e and 5f, the corresponding ARPES constant energy maps collected at the Fermi level, i.e. the Fermi surfaces, and at different binding energies are shown. For free standing graphene the electron density (n) in the conduction band is:

$$n = \frac{N}{A} = 2\ \frac{S_k}{4\pi^2}$$

where A is the graphene area, N the number of filled states in the π^* conduction band and S_k is the area in the first Brillouin zone occupied by populated conduction band electron states[36]. In our experiment, we are neglecting a trigonal warping for S_k observed for high degree of doping[36] in graphene and we are assuming a circular shape for the Fermi surface, reasonable for a low electron doping. Therefore, to carefully extract the surface pockets radius, we have taken the line profile of the photoemission intensity versus the k-momentum at the Fermi level and we have fitted it by two gaussian functions (Fig. 5a and 5b). Here, the estimated values of the electron density are n = (5.25 ± 0.12) ·10^{12} cm^{-2} for pristine graphene-SiC, and n = (5.73 ± 0.31) ·10^{12} cm^{-2} for the grafted sample. Considering the variation of the charge carrier density from the pristine graphene-SiC and the TMeOP-grafted sample (Δn = 0.48 ·10^{12} cm^{-2}), and the grafted molecular density ρ = 2.5 · 10^{-3} molecules · nm^{-2} (0.25 · 10^{12} molecules/cm^2) measured by STM measurements, we are able to estimate an upper limit of electrons donated by the molecules. This value sets that two electrons, which have been transferred from the TMeOP-grafted units to graphene-SiC (see Supplementary Information† for details on the charge transfer calculation). We regards this value as an upper estimation of the electrons transferred

from the molecules to graphene since it can be influenced by the total density of the grafted units.

Materials and methods

Epitaxial graphene on 6H-SiC(0001) purchased from Graphene supermarket was annealed in UHV (*10 $^{-10}$ mbar*) at 600^0 C for 30-60 mins in order to remove oxide impurities prior to measuring pristine graphene ARPES spectra.

Electrochemical measurements were performed using an Autolab PGSTAT101 potentiostat (Metrohm Autolab BV, The Netherlands). The electrochemical modification procedure was carried out in a homemade single-compartment three–electrode cell with a working electrode area of 12.5 mm^2, a Pt wire counter electrode and an Ag/AgCl (3M NaCl) reference electrode. 3,4,5-trimethoxybenzenediazonium (TMeOD) chloride salts are unstable and decompose rapidly: hence they were synthesized from the corresponding aniline precursor immediately prior to electrochemical reduction. This procedure involves 1 mM 3,4,5-trimethoxyaniline (97%, Sigma-Aldrich) with 0.1 M tetra-n-butylammonium hexafluorophosphate (98%, Acros) which was dissolved in 5 mL acetonitrile (99.9+%, Acros). For initiation of the diazotization reaction we first added boron trifluoride etherate to the aniline solution. This mixture was gently shaken for 5-10 seconds. Subsequently, we added the tert-butyl nitrite (90%, Acros) and the solution was shaken once more for 10-15 seconds. Finally, the solution was poured into the teflon EC cell. Cyclic voltammetry was used for the electrochemical activation (Supplementary Information, Fig. S3†). After modification, the TMeOP modified graphene samples were rinsed with acetonitrile to remove any physisorbed material from the surface and dried in an argon stream.

In order to prevent molecule desorption, the X-ray photoemission measurements have been performed after an annealing treatment of the samples at temperatures lower than 120°C in ultra-high vacuum conditions. Core level spectra have been collected at 30° emission angle with respect to the surface normal, with a properly calibrated[37] VG-SCIENTA R3000 analyzer, using the Al Kα line of a twin anode X-ray source operating at a base pressure of 2x10^{-10} torr. Angle-resolved valence band spectra were carried out at the BaDElPh beamline of the Elettra synchrotron in Trieste (Italy) using a photon energy of 34 eV, with p and s polarization, and a hemispherical electron analyzer SPECS Phoibos 150 with a 2D-CCD detector system[38]. Also the ARPES data were collected with the sample at room temperature (RT) and the images shown below are obtained summing the data acquired with both p and s polarization. We have acquired ARPES maps of the as-prepared functionalized sample, i.e. without undergoing any annealing treatment, and after annealing at 140°C and 220°C.

The STM measurements of the sample after an annealing at 80°C and 220°C in UHV, were collected in ambient conditions and at RT with an Agilent 5500 apparatus, the parameter of bias and current used for the measurements were in a range of (-0.3; -0.6) V and (30; 50) pA, respectively.

Raman measurements were performed with an OmegaScope 1000 (AIST-NT) with 632.8 nm He–Ne laser. The laser light was reflected by a long pass dichroic beam splitter (Chroma Technology Corporation, Z633RDC) and then was focused onto the sample surface through an objective (MITUTOYO, BD Plan Apo 100×, N.A. 0.7) with 500 kW cm^{-2} optical density at the sample surface. Raman scattering was collected and directed to a Raman spectrograph (HoribaJY, iHR-320) equipped with a cooled-charge coupled device (CCD) camera operated at −100 °C (Andor Technology, DU920P) through the dichroic mirror, a pinhole and long pass filter (Chroma Technology Corporation, HQ645LP). Each spectrum was taken for 10 seconds of accumulation time repeated 6 times. The samples were analysed at different focus point in order to obtain spectra of top graphene layer and underlying SiC substrate. The spectra acquired at the top of samples were normalized subtracted from SiC spectra in order to obtain only graphene spectra[39].

Conclusions

We have investigated the changes in the electronic band structure of graphene introduced by randomly TMeOP-grafted units. By STM images, XPS and Raman measurements we have confirmed the covalent functionalization of graphene by aryl radicals. These grafted units introduced a further n-type doping of graphene due a charge transfer from the molecules to graphene. The covalent modification with diazonium units is confirmed to preserve the electronic structure of graphene, as the value of the Fermi velocity along the high symmetry directions before and after the covalent modification does not change. These results pave the way to the possibility to tune, in a controlled way, the doping of graphene by dosing the quantity of the TMeOP-grafted molecules in the electrochemical solutions.

Conflicts of interest

There are not conflict of interests to declare.

Acknowledgements

S. P. acknowledges partial support from D.2.2 grants of the Università Cattolica del Sacro Cuore. The KU Leuven authors gratefully acknowledge financial support from the Fund of Scientific Research Flanders (FWO), KU Leuven - Internal Funds. The research leading to these results has also received funding from the European Research Council under the European Union's Seventh Frame-work Programme (FP7/2007-2013)/ERC Grant Agreement No. 340324 to S.D.F. We acknowledge Elettra Sincrotrone Trieste for providing access to its synchrotron radiation facilities and we thank L. Sancin for the technical assistance.

References

1. J. Liu, J. Tang and J. J. Gooding, *J. Mater. Chem.*, 2012, **22**, 12435.

2. V. P. Pham, H. S. Jang, D. Whang and J. Y. Choi, *Chemi. Soc. Rev.*, 2017, **46**, 6276-6300.
3. K. Khan, A. K. Tareen, M. Aslam, Y. Zhang, R. Wang, Z. Ouyang, Z. Gou and H. Zhang, *Nanoscale*, 2019, **11**, 21622-21678.
4. V. Georgakilas, M. Otyepka, A. B. Bourlinos, V. Chandra, N. Kim, K. C. Kemp, P. Hobza, R. Zboril and K. S. Kim, *Chem. Rev.*, 2012, **112**, 6156-6214.
5. G. Bottari, M. Á. Herranz, L. Wibmer, M. Volland, L. Rodríguez-Pérez, D. M. Guldi, A. Hirsch, N. Martín, F. D'Souza and T. Torres, *Chemical Society Reviews*, 2017, **46**, 4464-4500.
6. K. S. Mali, J. Greenwood, J. Adisoejoso, R. Phillipson and S. De Feyter, *Nanoscale*, 2015, **7**, 1566-1585.
7. L. Daukiya, M. N. Nair, M. Cranney, F. Vonau, S. Hajjar-Garreau, D. Aubel and L. Simon, *Progress in Surface Science*, 2019, **94**, 1-20.
8. S. Niyogi, E. Bekyarova, M. E. Itkis, H. Zhang, K. Shepperd, J. Hicks, M. Sprinkle, C. Berger, C. N. Lau, W. A. deHeer, E. H. Conrad and R. C. Haddon, *Nano Lett.*, 2010, **10**, 4061-4066.
9. A. Criado, M. Melchionna, S. Marchesan and M. Prato, *Angew. Chem. Int. Ed.*, 2015, **54**, 10734-10750.
10. M. Pykal, P. Jurecka, F. Karlicky and M. Otyepka, *Phys. Chem. Chem. Phys.*, 2016, **18**, 6351-6372.
11. A. Markevich, S. Kubasch, O. Lehtinen, O. Reimar, X. Feng, K. Mullen, A. Turchanin, A. N. Khlobystov, U. Kaiser and E. Besley, *Nanoscale*, 2016, **8**, 2711.
12. C. K. Chua and M. Pumera, *Chemi. Soc. Rev.*, 2013, **42**, 3222-3233.
13. J. Greenwood, T. H. Phan, Y. Fujita, Z. Li, O. Ivasenko, W. Vanderlinden, H. Van Gorp, W. Frederickx, G. Lu, K. Tahara, Y. Tobe, I. H. Uji, S. F. Mertens and S. De Feyter, *ACS nano*, 2015, **9**, 5520-5535.
14. M. Delamar, R. Hitmi, J. Pinson and J. M. Savbnt, *J. Am. Chem. Soc.*, 1992, **114**, 5884-5886.
15. K. Tahara, Y. Kubo, B. Lindner, S. Hashimoto, S. Hirose, A. Brown, B. Hirsch, L. Daukiya, S. De Feyter and Y. Tobe, *Langmuir : the ACS journal of surfaces and colloids*, 2019, **35**, 2089-2098.
16. S. Niyogi, E. Bekyarova, M. E. Itkis, H. Zhang, K. Shepperd, J. Hicks, M. Sprinkle, C. Berger, C. N. Lau, W. A. deHeer, E. H. Conrad and R. C. Haddon, *Nano Letters*, 2010, **10**, 4061-4066.
17. S. Niyogi, E. Bekyarova, J. Hong, S. Khizroev, C. Berger, W. de Heer and R. C. Haddon, *J. Phys. Chem. Lett.*, 2011, **2**, 2487-2498.
18. A. C. Ferrari, J. C. Meyer, V. Scardaci, C. Casiraghi, M. Lazzeri, F. Mauri, S. Piscanec, D. Jiang, K. S. Novoselov, S. Roth and A. K. Geim, *Phys. Rev. Lett.*, 2006, **97**, 187401.
19. L. G. Cançado, A. Jorio, E. H. Ferreira, F. Stavale, C. A. Achete, R. B. Capaz, M. V. Moutinho, A. Lombardo, T. S. Kulmala and A. C. Ferrari, *Nano Lett.*, 2011, **11**, 3190-3196.
20. D. Ferrah, J. Penuelas, C. Bottela, G. Grenet and A. Ouerghi, *Surf. Sci.*, 2013, **615**, 47-56.
21. C. Riedl, C. Coletti and U. Starke, *J.Phys. D: Appl. Phys.*, 2010, **43**, 374009.
22. L. Daukiya, C. Mattioli, D. Aubel, S. Hajjar-Garreau, F. Vonau, E. Denys, G. Reiter, J. Fransson, E. Perrin, M. L. Bocquet, C. Bena, A. Gourdon and L. Simon, *ACS nano*, 2017, **11**, 627-634.
23. C Riedl, C Coletti and U. Starke, *J. Phys. D: Appl. Phys.*, 2010, **43**, 374009.
24. C. Xia, L. I. Johansson, Y. Niu, A. A. Zakharov, E. Janzén and C. Virojanadara, *Carbon*, 2014, **79**, 631-635.
25. T. O. Wehling, A. M. Black-Schaffer and A. V. Balatsky, *Adv. Phys.*, 2014, **63**, 1-76.
26. S. Kim, J. Ihm, H. J. Choi and Y. W. Son, *Phys. Rev. Lett.*, 2008, **100**, 176802.
27. S. Y. Zhou, G. H. Gweon, A. V. Fedorov, P. N. First, W. A. De Heer, D. H. Lee, F. Guinea, A. H. Castro Neto and A. Lanzara, *Nat. Mater.*, 2007, **6**, 770-775.
28. R. A. Bueno, J. I. Martinez, R. F. Luccas, N. R. Del Arbol, C. Munuera, I. Palacio, F. J. Palomares, K. Lauwaet, S. Thakur, J. M. Baranowski, W. Strupinski, M. F. Lopez, F. Mompean, M. Garcia-Hernandez and J. A. Martin-Gago, *Nat. Commun.*, 2017, **8**, 15306.
29. S. Gottardi, K. Muller, L. Bignardi, J. C. Moreno-Lopez, T. A. Pham, O. Ivashenko, M. Yablonskikh, A. Barinov, J. Bjork, P. Rudolf and M. Stohr, *Nano Lett.*, 2015, **15**, 917-922.
30. F. Schedin, A. K. Geim, S. V. Morozov, E. W. Hill, P. Blake, M. I. Katsnelson and K. S. Novoselov, *Nat. Mater.*, 2007, **6**, 652-655.
31. S. Y. Zhou, D. A. Siegel, A. V. Fedorov and A. Lanzara, *Phys. Rev. Lett.*, 2008, **101**, 086402.
32. T. O. Wehling, K. S. Novoselov, S. V. Morozov, E. E. Vdovin, E. V. Katsnelson, A. K. Geim and A. I. and Lichtenstein, *Nano Lett.*, 173-177.
33. E. Bekyarova, M. E. Itkis, P. Ramesh, C. Berger, M. Sprinkle, W. A. De Heer and R. C. Haddon, *JACS Comm.*, 2009, **131**, 1336-1337.
34. G. Ambrosio, G. Drera, G. Di Santo, L. Petaccia, L. Daukiya, A. Brown, B. Hirsch, S. De Feyter, L. Sangaletti and S. Pagliara, *Sci. Rep. Submitted*.
35. C. Hansch, A. Leo and R. W. Taft, *Chem. Rev.*, 1991, **91**, 165-195.
36. A. V. Fedorov, N. I. Verbitskiy, D. Haberer, C. Struzzi, L. Petaccia, D. Usachov, O. Y. Vilkov, D. V. Vyalikh, J. Fink, M. Knupfer, B. Buchner and A. Gruneis, *Nat. Comm.*, 2014, **5**, 3257.
37. G. Drera, G. Salvinelli, J. Åhlund, P. G. Karlsson, B. Wannberg, E. Magnano, S. Nappini and L. Sangaletti, *J. Elec. Spec. and Rel. Phen.*, 2014, **195**, 109-116.
38. L. Petaccia, P. Vilmercati, S. Gorovikov, M. Barnaba, A. Bianco, D. Cocco, C. Masciovecchio and A. Goldoni, *Nucl. Instr. and Met. in Phys. Res. Sec. A*, 2009, **606**, 780-784.
39. L. Daukiya, *PhD Thesis Université de Haute-Alsace et Albert Ludwing Universität Freiburg*, 2016.